Supersensitization of CdS Quantum Dots with a Near-Infrared Organic Dye: Toward the Design of Panchromatic Hybrid-Sensitized Solar Cells

Hyunbong Choi,[†] Roxana Nicolaescu,[†] Sanghyun Paek,[‡] Jaejung Ko,[‡,*] and Prashant V. Kamat[†,*]

[†]Radiation Laboratory and Department of Chemistry and Biochemistry, University of Notre Dame, Notre Dame, Indiana 46556, United States and
[‡]Department of Advanced Material Chemistry, Korea University, Jochiwon, Chungnam 339-700, Korea

ABSTRACT The photoresponse of quantum dot solar cells (QDSCs) has been successfully extended to the near-IR (NIR) region by sensitizing nanostructured TiO_2—CdS films with a squaraine dye (JK-216). CdS nanoparticles anchored on mesoscopic TiO_2 films obtained by successive ionic layer adsorption and reaction (SILAR) exhibit limited absorption below 500 nm with a net power conversion efficiency of ~1% when employed as a photoanode in QDSC. By depositing a thin barrier layer of Al_2O_3, the TiO_2—CdS films were further modified with a NIR absorbing squaraine dye. Quantum dot sensitized solar cells supersensitized with a squariand dye (JK-216) showed good stability during illumination with standard global AM 1.5 solar conditions, delivering a maximum overall power conversion efficiency (η) of 3.14%. Transient absorption and pulse radiolysis measurements provide further insight into the excited state interactions of squaraine dye with SiO_2, TiO_2, and TiO_2/CdS/Al_2O_3 films and interfacial electron transfer processes. The synergy of combining semiconductor quantum dots and NIR absorbing dye provides new opportunities to harvest photons from different regions of the solar spectrum.

KEYWORDS: quantum dot solar cells · squaraine dye · photosensitization · transient absorption spectroscopy · pulse radiolysis · photocurrent generation · CdS

Quantum dot-sensitized solar cells have emerged as viable candidates to develop the next generation of energy conversion devices.[1−7] The ability to tune the effective band gap by size control of quantum dots (QDs),[8−11] harvest hot electrons,[12−14] and generate multiple charge carriers[15−17] with high-energy photons offers new ways to attain greater power conversion efficiencies. Of particular interest are the photoelectrochemical cells that employ size-quantized metal chalcogenides (e.g., CdS, CdSe, Sb_2S_3) anchored on mesoscopic TiO_2 films as photoanodes.[18−27] As the photogenerated electrons are captured and transported through the TiO_2 particle network, the holes are scavenged by a redox couple, such as a sulfide/polysulfide.[28] Decreasing particle size of quantum dots increases the charge injection rate into the TiO_2, but the increased band gap excludes longer wavelength absorption.[8,9,29] Although short-band gap quantum dots, such as PbS and PbSe, can harvest visible light energy, their performance in liquid junction solar cells is relatively low.[2,30]

Quantum dot solar cells (QDSCs), which typically exhibit power conversion efficiency in the range of 2−5%,[31−37] have yet to deliver efficiencies that are comparable to their counterpart, dye sensitized solar cells.[38−41] The factors that limit overall power conversion efficiency of QDSCs include limited absorption of the incident light, slow hole transfer rate, back electron transfer to the oxidized form of the redox couple, and low fill factors arising from poor counter electrode performance. To date, the sulfide/polysulfide redox couple has been the choice for most liquid junction QDSCs as it provides desirable stability during irradiation. Slow hole regeneration and anodic corrosion of the QDs limits the use of other common redox couples such as I^-/I_3^-.[42,43]

One approach to maximize the absorption of incident photons in QDSC is to couple different light absorbing components such that a good spectral match with visible and near-IR region of the solar radiation could be achieved. Supersensitization of QDs (e.g., CdS) with an organic dye absorbing in the infrared region provides a good combination to elucidate the feasibilty of this concept. Recently, Zaban et al.[44,45] reported the CdS quantum dot-TiO_2-dye(N719) bilayer cosensitization that facilitated the use of the I^-/I_3^- couple. In addition to significant overlap between the absorption of CdS and N719 dye, the reported power conversion efficiencies remained low. In order to demonstrate the concept of supersensitization in QDSC, we have now employed a squaraine

* Address correspondence to pkamat@nd.edu, jko@korea.ac.kr.

Received for review September 12, 2011 and accepted September 30, 2011.

Published online September 30, 2011
10.1021/nn2035022

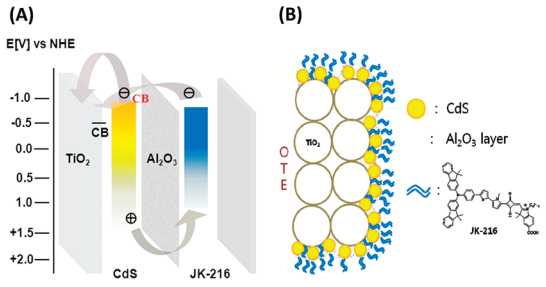

Scheme 1. (A) Charge-Transfer Process in Multilayer Supersensitized Nanocrystalline TiO_2 Film; (B) Schematic Drawing of TiO_2/CdS/Al_2O_3/JK-216 System

dye that selectively captures photons in the near-infrared (NIR) region and CdS QD that absorbs in the visible region (Scheme 1). The NIR squaraine dye (JK-216)[46] used in the present study serves dual purpose. First, the dye captures IR photons, and it scavenges holes from the CdS QDs, given that the valence band energy level of CdS is more positive than the highest occupied molecular orbital (HOMO) level of JK-216. The results that describe the QDSC performance and the interfacial electron transfer kinetics using transient spectroscopy are presented.

Extending the Photoresponse of CdS with JK-216. The mesoscopic TiO_2 films (4 μm thick) were modified with CdS (SILAR method) and JK-216 dye. In addition the dye was also anchored on an Al_2O_3 barrier layer deposited on CdS. The absorption spectra of CdS, JK-216, CdS/JK-216 and CdS/Al_2O_3/JK-216 deposited on TiO_2 film are shown in Figure 1. The absorption spectra of CdS show absorption below 510 nm corresponding to its band-gap of ~2.4 eV with a shoulder around 450 nm. JK-216 exhibits a prominent band in the red-near IR region with maximum at 660 nm. The dye exhibits relatively little absorption in the 400−500 nm region. The absorption spectra of CdS/JK-216 and CdS/Al_2O_3/JK-216 exhibit strong absorption bands corresponding to both CdS and dye. The prominent absorption band in the red region indicates strong adsorption of the dye onto these films. The high optical density of the CdS/Al_2O_3/JK-216 film as compared to CdS/JK-216 arises from the greater adsorption of the dye adsorption onto Al_2O_3 layer. Earlier studies that employed Al_2O_3 as a barrier layer in DSSC have also noted similar dye adsorption.[47,48]

Evaluation of QDSC Performance. The photoelectrochemical performance of mesoscopic TiO_2 films modified with CdS, JK-216, CdS/JK-216, and CdS/Al_2O_3/JK-216 was monitored under AM 1.5 irradiation (100 mW cm^{-2}) using a redox couple, 0.22 M $Co(bpy)_3(PF_6)_2$, 0.033 M $Co(bpy)_3(PF_6)_3$, 0.1 M $LiClO_4$, and 0.2 M 4-*tert*-butylpyridine in acetonitrile. Figure 2A shows the incident phototo-current conversion effficiency (IPCE) of QDSCs based on CdS, JK-216, CdS/JK-216, and CdS/Al_2O_3/JK-216. The TiO_2/CdS electrode responds only below 500 nm. The electrodes modified with the dye show two maxima around 450 and 660 nm, thus

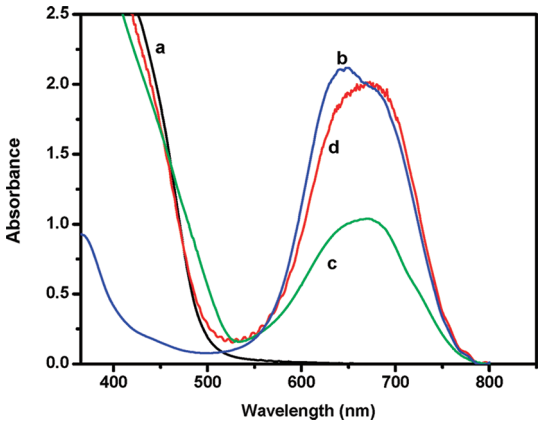

Figure 1. Absorption spectra of (a) CdS, (b) JK-216, (c) CdS/JK-216, and (d) CdS/Al_2O_3/JK-216 adsorbed onto TiO_2 films.

confirming the participation of both the CdS and dye molecules in the overall photocurrent generation process. The maximum IPCE observed for the CdS/Al_2O_3/JK-216 cell was about 67% at 450 nm, significantly higher than TiO_2/CdS (~45%). The IPCE of 10−30% in the red-near IR region shows the extended response of the QDSC up to 800 nm.

Comparison of IPCE spectra at 450 nm (CdS absorption region) shows an interesting dependence of the cell response to the presence of JK-216. The IPCE values measured at 450 nm of CdS, CdS/JK-216, and CdS/Al_2O_3/JK-216 were 47, 50, and 67%, respectively. It should be noted that the absorbances at 450 nm of CdS, CdS/JK-216, and CdS/Al_2O_3/JK-216 were maintained constant at 1.50 ± 0.05. Hence, the difference in IPCE cannot be attributed to a varying degree of light absorption by the CdS. This synergy between the CdS and the dye in facilitating higher photocurrent generation indicates an additional role of the dye in shuttling holes across the CdS/dye−electrolyte interface. This electron shuttling aspect is similar to that observed with a C_{60}/C_{60}^- couple deposited on a TiO_2/Ru(II) complex in a dye sensitized solar cell.[49]

With TiO_2 films modified with JK-216 alone, we observe photocurrent (spectrum b in Figure 2) arising from the dye sensitization process (reactions 1 and 2)

$$\text{dye} + h\nu \rightarrow {}^1\text{dye}^* \quad (1)$$

$${}^1\text{dye}^* + \text{TiO}_2 \rightarrow \text{dye}^{\bullet+} + \text{TiO}_2(\text{e}) \quad (2)$$

In the case of CdS (spectrum a in Figure 2) reactions 3 and 4 and CdS/JK-216 (spectrum c, in Figure 2) reactions 3−6 contribute to the overall photocurrent generation.

$$\text{CdS} + h\nu \rightarrow \text{CdS}(\text{e} + \text{h}) \quad (3)$$

$$\text{CdS}(\text{e}) + \text{TiO}_2 \rightarrow \text{CdS} + \text{TiO}_2(\text{e}) \quad (4)$$

$$\text{CdS}(\text{h}) + \text{dye} \rightarrow \text{CdS} + \text{dye}^{\bullet+} \quad (5)$$

$$\text{dye}^{\bullet+} + \text{Co(III)} \rightarrow \text{dye} + \text{Co(II)} \quad (6)$$

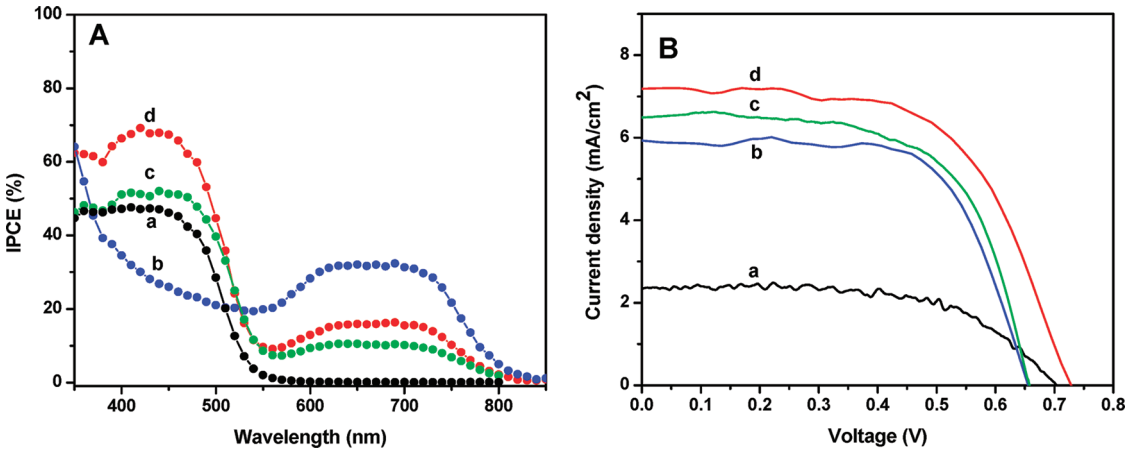

Figure 2. (A) IPCE spectra and (B) $J-V$ curves recorded for nanostructured TiO_2 film electrodes modified with (a) CdS, (b) JK-216, (c) CdS/JK-216, and (d) CdS/Al_2O_3/JK-216. (Electrolyte: 0.22 M $Co(bpy)_3(PF_6)_2$, 0.033 M $Co(bpy)_3(PF_6)_3$, 0.1 M $LiClO_4$, and 0.2 M 4-*tert*-butylpyridine in acetonitrile).

TABLE 1. DSSC Performance Parameters of Dyes[a]

dye	J_{sc} (mA cm^{-2})	V_{oc} (V)	FF	η (%)
CdS	2.341	0.704	0.62	1.01
JK-216	5.932	0.65	0.67	2.59
CdS/JK-216	6.489	0.657	0.66	2.80
CdS/Al_2O_3/JK-216	7.186	0.728	0.60	3.14

[a] Performances of DSSCs were measured with 0.18 cm^2 working area. Electrolyte: 0.22 M $Co(bpy)_3(PF_6)_2$, 0.033 M $Co(bpy)_3(PF_6)_3$, 0.1 M $LiClO_4$, and 0.2 M 4-*tert*-butylpyridine in acetonitrile.

Evidence for the hole transfer reaction (reaction 5) was independently obtained from transient absorption spectroscopy and this will be discussed in the latter part of this paper.

The $I-V$ characteristics of the QDSC employing various photoanodes are presented in Figure 2B. The short-circuit current density (J_{sc}), open-circuit voltage (V_{oc}), fill factor (FF), and overall conversion efficiency (η) of CdS/Al_2O_3/JK-216 are 7.18 mA cm^{-2}, 728 mV, 0.60, and 3.14%, respectively. For CdS/JK-216, the photovoltaic parameters are 6.48 mA cm^{-2}, 657 mV, 0.66, and 2.80%, respectively. The improvement in the cell performance resulting from the modifications in the architecture is evident from the results summarized in Table 1. There is a 70 mV increase in V_{oc} of the CdS/Al_2O_3/JK-216 cell under illumination compared to CdS/JK-216. This significant increase in V_{oc} suggests that the Al_2O_3 layer suppresses the recombination reaction between the oxidized dye and injected electron at the CdS interface. In addition to increased V_{oc}, we also noted a significant increase in the short circuit current. J_{sc} of CdS/Al_2O_3/JK-216 cell is 3 times higher than the CdS cell. This high current is attributed to the increased spectral response of the cell containing the dye as well as enhanced electron–hole separation *via* dye scavenging.

In addition to increased photoelectrochemical performance of the CdS/Al_2O_3/JK-216 electrode, the

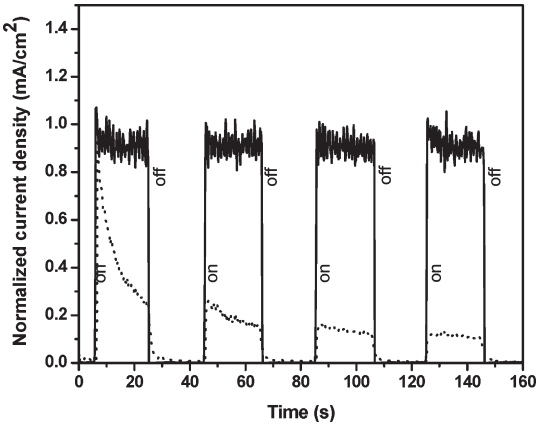

Figure 3. Photocurrent response of CdS/Al_2O_3 (dashed line) and CdS/Al_2O_3/JK-216 (solid line) electrode under AM 1.5 sunlight in cobalt based electrolyte. Electrolyte: 0.22 M $Co(bpy)_3(PF_6)_2$, 0.033 M $Co(bpy)_3(PF_6)_3$, 0.1 M $LiClO_4$, and 0.2 M 4-*tert*-butylpyridine in acetonitrile.

photochemical stabilization of CdS is seen with JK-216 dye. Figure 3 shows the photocurrent response to on–off cycles of illumination of a photoelectrochemical cell with CdS/Al_2O_3 and CdS/Al_2O_3/JK-216 as anodes. The photocurrents were normalized to the first cycle of illumination. Whereas the CdS/Al_2O_3/JK-216 electrode shows stable behavior, the CdS electode alone undergoes continuous decrease of the current, indicating a progressive degradation of CdS in the presence of the Co(II)/Co(III) redox couple. These results further point out the beneficial aspect of JK-216 in stabilizing the CdS against anodic photocorrosion by scavenging the photogenerated holes (reactions 5 and 6).

Mechanistic Insights into the Role of JK-216 Dye. As observed from the photoelectrochemical behavior of the squaraine dye modified TiO_2 and TiO_2/CdS film, the dye, JK-216, plays two different roles. (i) On the TiO_2 surface, the dye injects electrons from the excited state to produce dye$^{\bullet+}$ as a reaction intermediate (reaction 2).

(ii) On the CdS surface its major role is to scavenge photogenerated holes to produce dye$^{\bullet+}$ (reaction 5). In both of these reaction pathways, the reaction intermediate is the dye cation radical. We employed femtosecond transient absorption spectroscopy and pulse radiolysis to establish the formation of the dye$^{\bullet+}$. Figure 4A shows time-resolved transient absorption spectra recorded following 387 nm laser pulse excitation of JK-216 adsorbed onto a mesoscopic SiO_2 film and a TiO_2 film. Since the dye is the only absorber at the excitation wavelength, we can follow the deactivation of the excited dye by these two processes. Since SiO_2 is an insulator, it serves as a neutral substrate, not directly participating in any electron transfer process. The observed spectral characteristics correspond to the singlet excited dye. The difference spectrum of the singlet excited dye exhibits a broad absorption maximum around 530 nm and a strong bleaching in the region of the ground-state absorption (600−700 nm region). From the exponential decay of the transient, the singlet excited state lifetime is calculated to be about 25 ps.

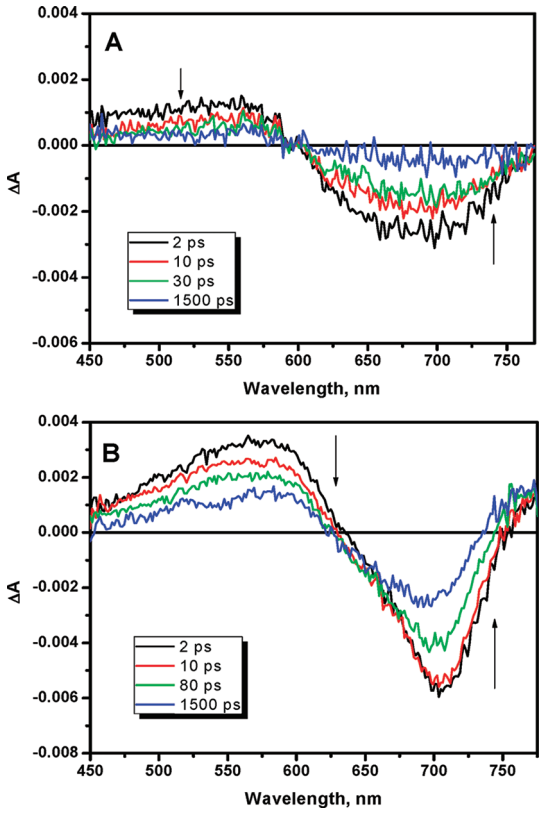

Figure 4. Differential absorption spectra obtained upon femtosecond flash photolysis (387 nm) of JK-216 adsorbed onto the (A) SiO_2 film and (B) TiO_2 film.

On the other hand, the difference absorption spectra recorded following laser pulse excitation of the dye adsorbed on the TiO_2 film exhibit two absorption maxima at 580 nm and >760 nm accompanied by the bleaching around 660 nm (Figure 4B). This transient is long-lived and contrasts in spectral characteristics to that observed with SiO_2 film in Figure 5A. We observe about 50% decay during the monitoring time of 1.6 ns. We attribute this transient to the oxidized state of the dye$^{\bullet+}$ formed as a result of charge injection from the excited dye into TiO_2 surface. Since we observe this transient within 1 ps following the laser pulse excitation, we expect the charge transfer rate constant to be $\sim 10^{12}$ s^{-1}.

We have independently confirmed the spectral identity of dye$^{\bullet+}$ using pulse radiolysis experiments. Solutions of JK-216 in O_2-saturated methylene chloride were subjected to electron pulse irradiation to generate the dye$^{\bullet+}$ radical. Methylene chloride was used as the solvent for pulse radiolysis since it provides good solubility for JK-216 as well as the posibility of generating a predominantly oxidizing environment during the experiment.[50,51] Similar methods have also been successfully adopted to characterize other squaraine dyes.[52−54]

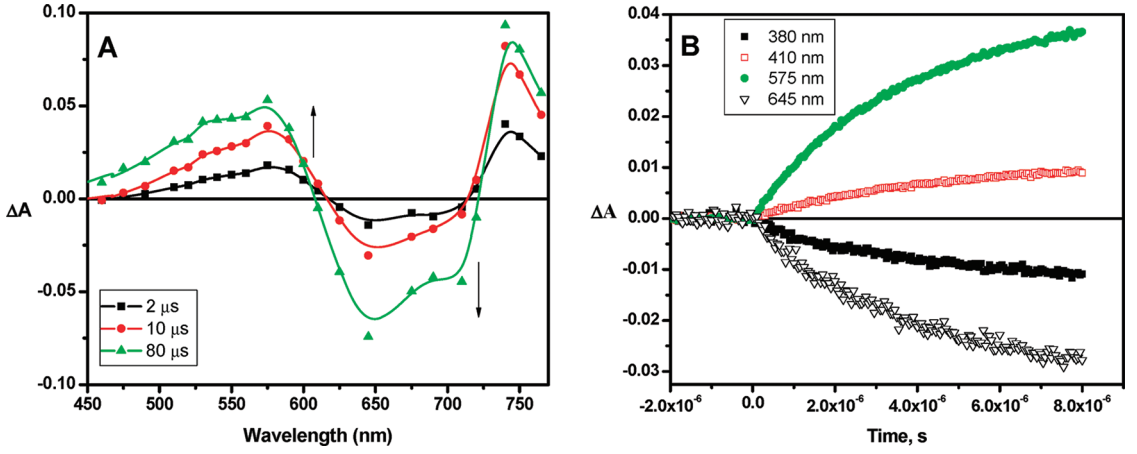

Figure 5. (A) Time resolved absorption spectra obtained during the pulse radiolysis of JK-216 solution in oxygenated methylene chloride. (B) The build-up traces of the transient specie(s) and decay of the ground state.

The radiolysis of methylene chloride leads to the carbon centered radicals, $^{\bullet}CH_2Cl$ and $^{\bullet}CHCl_2$:

$$CH_2Cl_2 \rightarrow e^-_{sol} + (CH_2Cl_2)^{\bullet+} \quad (7)$$

$$CH_2Cl_2 + e^-_{sol} \rightarrow {}^{\bullet}CH_2Cl + Cl^- \quad (8)$$

In oxygenated solutions, the chloromethyl and dichloromethyl radicals rapidly react to yield the respective oxidizing peroxy radicals, $^{\bullet}OOCH_2Cl$. These peroxyl radicals further react by oxidizing the JK-216 dye.

$$^{\bullet}CH_2Cl + O_2 \rightarrow {}^{\bullet}OOCH_2Cl \quad (9)$$

$$dye + {}^{\bullet}OOCH_2Cl \rightarrow CH_2ClO_2^- + dye^{\bullet+} \quad (10)$$

Time-resolved transient absorption spectra recorded following the pulse irradiation of JK-216 in O_2 saturated CH_2Cl_2 are shown in Figure 5A. The dye exhibits a broad absorption band in the 420−600 nm region, and one above 720 nm as well as strong bleach in the spectral range of the ground state absorption (620−700 nm). The buildup of the transient intermediate and the decay due to the depletion of the ground state shown in Figure 5B show similar growth kinetics. The observed transient absorption features match well with the spectra recorded for the TiO_2/JK-216 system in Figure 4B, thus confirming the identity of dye cation radical.

The question that remains to be answered is the hole-transfer from excited CdS to JK-216 in the supersensitized films (SiO_2/CdS/Al_2O_3/JK-216 and TiO_2/CdS/Al_2O_3/JK-216). Figure 6A shows the transient absorption spectra recorded following laser pulse excitation of SiO_2/CdS/Al_2O_3/JK-216. These spectra exhibit stong bleaching in the region of ground state excitonic band (490 nm) of CdS. The dominence of CdS bleaching ensures that the excitation is centered mainly at CdS. The contribution of the excited dye to the overall absorption spectra is small because of the low absorption of the dye as compared to CdS. The spectra in Figure 6A point out the existence of small absorption bands at 580 nm and at >750 nm indicating the formation of small amount of dye cation radical as a result of interaction between excited CdS and JK-216. The transient absorption at 580 and 760 nm is prominently seen when CdS/JK-216 were deposited on TiO_2 films (Figure 6B). The close similarity between the difference spectra of TiO_2/JK-216 and TiO_2/CdS/Al_2O_3/JK-216 confirm the dye cation radical formation albeit the origin rests in different reaction pathways (viz., reactions 2 and 5).

In conclusion, we present a new design for the development of quantum dot sensitized solar cell

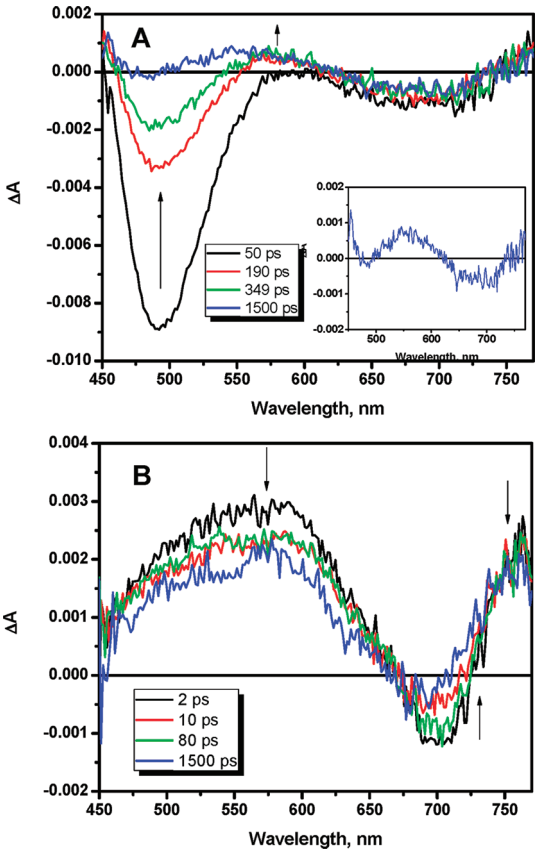

Figure 6. Differential absorption spectra obtained upon femtosecond flash photolysis (387 nm) of CdS/Al_2O_3/JK-216 absorbed onto (A) SiO_2 film and (B) TiO_2 film. The inset shows the difference absorption spectrum of CdS/Al_2O_3/JK-216 recorded at 1500 ps.

that couples semiconductor nanocrystal and a red-NIR organic dye with complementary spectral absorption in the visible region. Quantum dot sensitized solar cells with JK-216 show good stability using a cobalt-based electrolyte under illumination. In the presence of JK-216, the direct excitation of CdS leads to transfer of the hole from CdS to JK-216. We conclude that the use of JK-216 is energetically a good match to regenerate CdS by capturing photogenerated holes while concurrently serving as a sensitizer in the red-IR region. The introduction of a barrier layer is also crucial in maintaing the synergy between CdS and the dye and in enhancing the overall performance of QDSC. The results discussed here pave the way for the design of new, efficient quantum dot supersensitized solar cells with improved stability and absorption characteristics through the addition of a NIR dye.

EXPERIMENTAL METHODS

Materials. $Co(bpy)_3(PF_6)_2$, $Co(bpy)_3(PF_6)_3$ was synthesized using the procedure described in the literature.[55]

Optical and Electrochemical Measurements. All experiments were carried out at room temperature. All solutions were deaerated by bubbling with nitrogen or argon. Absorption spectra were measured with a Varian Cary 50-Bio UV−vis spectrophotometer.

A Princeton Applied Research model PARSTAT 2263 was used for recording $I-V$ characteristics. Newport Oriel QE Kit (QE–PV-SI) was used for measuring IPCE values.

Nanocrystalline TiO_2 Electrode Preparation. FTO glass plates (Pilkington TEC Glass-TEC 8, Solar 2.3 mm thickness) were cleaned in a detergent solution using an ultrasonic bath for 30 min, rinsed with water and ethanol. The FTO glass plates were immersed in 40 mM $TiCl_4$ (aqueous) at 70 °C for 30 min and washed with water and ethanol. A transparent nanocrystalline layer on the FTO glass plate was prepared by doctor blade printing TiO_2 paste (Solaronix, Ti-Nanoxide T/SP) and then dried at 25 °C for 2 h. The TiO_2 electrodes were gradually heated under an air flow at 325 °C for 5 min, at 375 °C for 5 min, at 450 °C for 15 min, and at 500 °C for 15 min. A paste for the scattering layer containing 400 nm sized anatase TiO_2 particles (CCIC, PST-400C) was deposited by doctor blade printing and then dried for 2 h at 25 °C. The TiO_2 electrodes were again gradually heated under an air flow at 325 °C for 5 min, at 375 °C for 5 min, at 450 °C for 15 min, and at 500 °C for 15 min. The TiO_2 electrodes were treated again by $TiCl_4$ at 70 °C for 30 min and sintered at 500 °C for 30 min.

CdS Deposition by Successive Ionic Layer Adsorption and Reaction (SILAR) Method. TiO_2 films prepared by the above-described procedure were successively exposed to $CdSO_4$ and Na_2S solutions to deposit CdS nanocrystallites. The TiO_2 electrodes were immersed in a solution of $CdSO_4$ (0.1 M) for 1 min. They were then rinsed with DI H_2O and immersed in a Na_2S (0.1 M) solution for another 1 min followed by another rinsing with DI water. This SILAR process was repeated 5 times.

TiO_2/CdS/Al_2O_3/JK-216 Samples. The TiO_2/CdS was immersed in a 15 mM aluminum isopropoxide solution in isopropanol for 15 min at room temperature. To achieve the hydrolysis of the aluminum ispropoxide, the film was exposed to ambient air for 20 min. The aluminum oxide coated TiO_2/CdS electrodes were then immersed into the JK-216 (0.1 mM in EtOH containing 20 mM 3a,7a-dihydroxy-5b-cholic acid (Cheno)) and kept at room temperature for 4 h.

TiO_2/CdS/JK-216 and TiO_2/JK-216 Samples. The TiO_2/CdS and TiO_2 electrodes were immersed into the JK-216 (0.1 mM in EtOH containing 20 mM 3a,7a-dihydroxy-5b-cholic acid (Cheno)) and kept at room temperature for 4 h.

Solar Cell Fabrication. The sensitized TiO_2 film is used as a working electrode. The FTO plate (Pilkington TEC Glass-TEC 8, Solar 2.3 mm thickness) used for the counter electrodes was cleaned with ultrasonic bath in H_2O, acetone, and 0.1 M HCl(aq), subsequently. Counter electrodes were prepared by coating with a drop of H_2PtCl_6 solution (2 mg of Pt in 1 mL of ethanol) on the cleaned FTO plate and sintered at 400 °C for 15 min. The dye adsorbed TiO_2 electrode and Pt-counter electrode were assembled into a sealed sandwich-type cell by heating at 80 °C with a hot-melt ionomer film (Surlyn SX 1170-25, Solaronix) as a spacer between the electrodes. A typical electrode area was in the range 0.25–0.3 cm^2. A drop of electrolyte solution (electrolyte of 0.22 M $Co(bpy)_3(PF_6)_2$, 0.033 M $Co(bpy)_3(PF_6)_3$, 0.1 M $LiClO_4$, and 0.2 M 4-*tert*-butylpyridine in acetonitrile) was placed over a hole drilled in the counter electrode of the assembled cell and was driven into the cell *via* vacuum backfilling. Finally, the hole was sealed using additional Surlyn and a cover glass (0.1 mm thickness).

Femtosecond Laser Flash Photolysis. Femtosecond transient absorption experiments were conducted using a CPA-2010 1 kHz amplified Ti:sapphire laser system from Clark MXR, combined with Helios optical detection system provided by Ultrafast Systems. The fundamental output of the CPA-2010 laser system (775 nm, 1 mJ per pulse, pulse width 150 fs) was split into two beams: a pump (95%) and a probe (5%). The pump beam was directed through a second harmonic generator to provide 387 nm excitation wavelength used in all of the experiments. The probe beam passed through an optical delay rail, allowing regulation of an appropriate delay time between the pump and the probe.

Nanosecond Pulse Radiolysis. Pulse radiolysis experiments were carried out using the Notre Dame 7-MeV Titan Beta model TBS-8/16-1S linear accelerator (LINAC), with a pulse length of 2.5 ns. Each experimental point is the average of at least five replicate shots using the continuous flow mode of the instrument. The dosimetry was carried out with N_2O-saturated solutions of 10 mM KSCN, based on the extinction coefficient for $(SCN)_2^{\bullet-}$ of $\varepsilon_{472\ nm} = 7580\ M^{-1}\ cm^{-1}$ and the radiation chemical yield $G = 6.13$. The G-value is defined as the number of species formed per 100 eV. The oxidation of the JK-216 was investigated in methylene chloride; the concentration of the JK-216 was 50 μM. Methylene chloride (Fisher) was HPLC grade. Analysis of optical absorption versus time was done using Origin (Microcal) software.

Acknowledgment. The research described herein was supported by the Department of Energy, Office of Basic Energy Sciences. This is contribution number NDRL 4899 from the Notre Dame Radiation Laboratory. The research described herein was supported by the Division of Chemical Sciences, Geosciences, and Biosciences, Office of Basic Energy Sciences of the U.S. Department of Energy through Award DE-FC02-04ER15533. H.C. and J.K. acknowledge the support of the WCU (The Ministry of Education and Science, Korea) Program (Grant No. R31-2008-000-10035-0) and the Converging Research Center Program through the National Research Foundation of Korea funded by the Ministry of Education, Science and Technology (Grant 2010K000973)

Supporting Information Available: Additional IPCE spectra comparing TiO_2 and TiO_2/Al_2O_3 electrodes. This material is available free of charge *via* the Internet at http://pubs.acs.org.

REFERENCES AND NOTES

1. Kamat, P. V. Quantum Dot Solar Cells. Semiconductor Nanocrystals as Light Harvesters. *J. Phys. Chem. C* **2008**, *112*, 18737–18753.
2. Kamat, P. V.; Tvrdy, K.; Baker, D. R.; Radich, J. G. Beyond Photovoltaics: Semiconductor Nanoarchitectures for Liquid Junction Solar Cells. *Chem. Rev.* **2010**, *110*, 6664–6688.
3. Nozik, A. J. Quantum Dot Solar Cells. *Physica E* **2002**, *14*, 115–120.
4. Yu, P.; Zhu, K.; Norman, A. G.; Ferrere, S.; Frank, A. J.; Nozik, A. J. Nanocrystalline TiO_2 Solar Cells Sensitized with InAs Quantum Dots. *J. Phys. Chem. B* **2006**, *110*, 25451–25454.
5. Hodes, G. Comparison of Dye- and Semiconductor-Sensitized Porous Nanocrystalline Liquid Junction Solar Cells. *J. Phys. Chem. C* **2008**, *112*, 17778–17787.
6. Mora-Sero, I.; Bisquert, J. Breakthroughs in the Development of Semiconductor Sensitized Solar Cells. *J. Phys. Chem. Lett.* **2010**, *1*, 3046–3052.
7. Palomares, E.; Martinez-Ferrero, E.; Albero, J. Materials, Nanomorphology and Interfacial Charge Transfer Reactions in Quantum Dot/Polymer Solar Cell Devices. *J. Phys. Chem. Lett.* **2010**, *1*, 3039–3045.
8. Kongkanand, A.; Tvrdy, K.; Takechi, K.; Kuno, M. K.; Kamat, P. V. Quantum Dot Solar Cells. Tuning Photoresponse through Size and Shape Control of CdSe-TiO_2 Architecture. *J. Am. Chem. Soc.* **2008**, *130*, 4007–4015.
9. Robel, I.; Kuno, M.; Kamat, P. V. Size-Dependent Electron Injection from Excited CdSe Quantum Dots into TiO_2 Nanoparticles. *J. Am. Chem. Soc.* **2007**, *129*, 4136–4137.
10. Wang, D. F.; Zhao, H. G.; Wu, N. Q.; El Khakani, M. A.; Ma, D. L. Tuning the Charge-Transfer Property of PbS-Quantum Dot/TiO_2-Nanobelt Nanohybrids *via* Quantum Confinement. *J. Phys. Chem. Lett.* **2010**, *1*, 1030–1035.
11. Choi, J. J.; Lim, Y.-F.; Santiago-Berrios, M. E. B.; Oh, M.; Hyun, B.-R.; Sun, L.; Bartnik, A. C.; Goedhart, A.; Malliaras, G. G.; Abruna, H. C. D.; et al. PbSe Nanocrystal Excitonic Solar Cells. *Nano Lett.* **2009**, *9*, 3749–3755.
12. Pandey, A.; Guyot-Sionnest, P. Hot Electron Extraction from Colloidal Quantum Dots. *J. Phys. Chem. Lett.* **2010**, *1*, 45–47.
13. Tisdale, W. A.; Williams, K. J.; Timp, B. A.; Norris, D. J.; Aydil, E. S.; Zhu, X. Y. Hot-Electron Transfer from Semiconductor Nanocrystals. *Science* **2010**, *328*, 1543–1547.
14. Sambur, J. B.; Novet, T.; Parkinson, B. A. Multiple Exciton Collection in a Sensitized Photovoltaic System. *Science* **2010**, *330*, 63–66.
15. Schaller, R. D.; Sykora, M.; Jeong, S.; Klimov, V. I. High-Efficiency Carrier Multiplication and Ultrafast Charge Separation in Semiconductor Nanocrystals Studied *via*

Time-Resolved Photoluminescence. *J. Phys. Chem. B* **2006**, *110*, 25332–25338.
16. Beard, M. C.; Knutsen, K. P.; Yu, P. R.; Luther, J. M.; Song, Q.; Metzger, W. K.; Ellingson, R. J.; Nozik, A. J. Multiple Exciton Generation in Colloidal Silicon Nanocrystals. *Nano Lett.* **2007**, *7*, 2506–2512.
17. Beard, M. C. Multiple Exciton Generation in Semiconductor Quantum Dots. *J. Phys.Chem. Lett.* **2011**, *2*, 1282–1288.
18. Kim, J. Y.; Choi, S. B.; Noh, J. H.; HunYoon, S.; Lee, S.; Noh, T. H.; Frank, A. J.; Hong, K. S. Synthesis of CdSe-TiO_2 Nanocomposites and Their Applications to TiO_2 Sensitized Solar Cells. *Langmuir* **2009**, *25*, 5348–5351.
19. Baker, D. R.; Kamat, P. V. Disassembly, Reassembly and Photoelectrochemistry of Etched TiO_2 Nanotubes. *J. Phys. Chem. C* **2009**, *113*, 17967–17972.
20. Bang, J. H.; Kamat, P. V. Quantum Dot Sensitized Solar Cells. A Tale of Two Semiconductor Nanocrystals: CdSe and CdTe. *ACS Nano* **2009**, *3*, 1467–1476.
21. Lee, H. J.; Yum, J. H.; Leventis, H. C.; Zakeeruddin, S. M.; Haque, S. A.; Chen, P.; Seok, S. I.; Gratzel, M.; Nazeeruddin, M. K. CdSe Quantum Dot-Sensitized Solar Cells Exceeding Efficiency 1% at Full-Sun Intensity. *J. Phys. Chem. C* **2008**, *112*, 11600–11608.
22. Wang, G. M.; Yang, X. Y.; Qian, F.; Zhang, J. Z.; Li, Y. Double-Sided CdS and CdSe Quantum Dot Co-Sensitized ZnO Nanowire Arrays for Photoelectrochemical Hydrogen Generation. *Nano Lett.* **2010**, *10*, 1088–1092.
23. Breus, V. V.; Heyes, C. D.; Nienhaus, G. U. Quenching of CdSe-ZnS Core-Shell Quantum Dot Luminescence by Water-Soluble Thiolated Ligands. *J. Phys. Chem. C* **2007**, *111*, 18589–18594.
24. Gao, X. F.; Sun, W. T.; Ai, G.; Peng, L. M. Photoelectric Performance of TiO_2 Nanotube Array Photoelectrodes Cosensitized with CdS/CdSe Quantum Dots. *Appl. Phys. Lett.* **2010**, *96*, art. no. 153104.
25. Lee, H.; Leventis, H. C.; Moon, S. J.; Chen, P.; Ito, S.; Haque, S. A.; Torres, T.; Nuesch, F.; Geiger, T.; Zakeeruddin, S. M.; et al. PbS and CdS Quantum Dot-Sensitized Solid-State Solar Cells: "Old Concepts, New Results. *Adv. Funct. Mater.* **2009**, *19*, 2735–2742.
26. Fuke, N.; Hoch, L. B.; Koposov, A. Y.; Manner, V. W.; Werder, D. J.; Fukui, A.; Koide, N.; Katayama, H.; Sykora, M. CdSe Quantum-Dot-Sensitized Solar Cell with ~100% Internal Quantum Efficiency. *ACS Nano* **2010**, *4*, 6377–6386.
27. Moon, S.-J.; Itzhaik, Y.; Yum, J.-H.; Zakeeruddin, S. M.; Hodes, G.; Gratzel, M. Sb_2S_3-Based Mesoscopic Solar Cell using an Organic Hole Conductor. *J. Phys. Chem. Lett.* **2010**, *1*, 1524–1527.
28. Chakrapani, V.; Baker, D.; Kamat, P. V. Understanding the Role of the Sulfide Redox Couple (S^{2-}/S_n^{2-}) in Quantum Dot Sensitized Solar Cells. *J. Am. Chem. Soc.* **2011**, *133*, 9607–9615.
29. Tvrdy, K.; Frantszov, P.; Kamat, P. V. Photoinduced Electron Transfer from Semiconductor Quantum Dots to Metal Oxide Nanoparticles. *Proc. Natl. Acad. Sci. U.S.A.* **2011**, *108*, 29–34.
30. Lee, H. J.; Chen, P.; Moon, S. J.; Sauvage, F.; Sivula, K.; Bessho, T.; Gamelin, D. R.; Comte, P.; Zakeeruddin, S. M.; Il Seok, S.; et al. Regenerative PbS and CdS Quantum Dot Sensitized Solar Cells with a Cobalt Complex as Hole Mediator. *Langmuir* **2009**, *25*, 7602–7608.
31. Diguna, L. J.; Shen, Q.; Kobayashi, J.; Toyoda, T. High Efficiency of CdSe Quantum-Dot-Sensitized TiO_2 Inverse Opal Solar Cells. *Appl. Phys. Lett.* **2007**, *91*, Article No. 023116
32. Shen, Q.; Kobayashi, J.; Diguna, L. J.; Toyoda, T. Effect of ZnS Coating on the Photovoltaic Properties of CdSe Quantum Dot-Sensitized Solar Cells. *J. Appl. Phys.* **2008**, *103*, Article No. 084304.
33. Barea, E. M.; Shalom, M.; Giménez, S.; Hod, I.; Mora-Seró, I. n.; Zaban, A.; Bisquert, J. Design of Injection and Recombination in Quantum Dot Sensitized Solar Cells. *J. Am. Chem. Soc.* **2010**, *132*, 6834–6839.
34. Gonzalez-Pedro, V.; Xu, X.; Mora-Sero, I.; Bisquert, J. Modeling High-Efficiency Quantum Dot Sensitized Solar Cells. *ACS Nano* **2010**, *4*, 5783–5790.
35. Pattantyus-Abraham, A. G.; Kramer, I. J.; Barkhouse, A. R.; Wang, X.; Konstantatos, G.; Debnath, R.; Levina, L.; Raabe, I.; Nazeeruddin, M. K.; Grätzel, M.; et al. Depleted-Heterojunction Colloidal Quantum Dot Solar Cells. *ACS Nano* **2010**, *4*, 3374–3380.
36. Chang, J. A.; Rhee, J. H.; Im, S. H.; Lee, Y. H.; Kim, H.-j.; Seok, S. I.; Nazeeruddin, M. K.; Gratzel, M. High-Performance Nanostructured Inorganic-Organic Heterojunction Solar Cells. *Nano Lett.* **2010**, *10*, 2609–2612.
37. Radich, J. G.; Dwyer, R.; Kamat, P. V. Cu_2S -Reduced Graphene Oxide Composite for High Efficiency Quantum Dot Solar Cells . Overcoming the Redox Limitations of S^{2-}/S_n^{2-} at the Counter Electrode. *J. Phys. Chem. Lett.* **2011**, *2*, 2453–2460.
38. Alstrum-Acevedo, J. H.; Brennaman, M. K.; Meyer, T. J. Chemical Approaches to Artificial Photosynthesis. *Inorg. Chem.* **2005**, *44*, 6802–6827.
39. Graetzel, M. Recent Advances in Sensitized Mesoscopic Solar Cells. *Acc. Chem. Res.* **2009**, *42*, 1788–1798.
40. Hagfeldt, A.; Boschloo, G.; Sun, L.; Kloo, L.; Pettersson, H. Dye-Sensitized Solar Cells. *Chem. Rev.* **2010**, *110*, 6595–6663.
41. Miyasaka, T. Toward Printable Sensitized Mesoscopic Solar Cells: Light-Harvesting Management with Thin TiO_2 Films. *J. Phys. Chem. Lett.* **2011**, *2*, 262–269.
42. Meyer, G. J.; Rowley, J.; Farnum, B.; Ardo, S. Making and Breaking I-I Bonds for Solar Energy Conversion. *J. Phys. Chem. Lett.* **2010**, *1*, 3132–3140.
43. Call, F.; Stolwijk, N. A. Impact of I_2 Additions on Iodide Transport in Polymer Electrolytes for Dye-Sensitized Solar Cells: Reduced Pair Formation versus a Grotthuss-Like Mechanism. *J. Phys. Chem. Lett.* **2010**, *1*, 2088–2093.
44. Shalom, M.; Albero, J.; Tachan, Z.; Martinez-Ferrero, E.; Zaban, A.; Palomares, E. Quantum Dot-Dye Bilayer-Sensitized Solar Cells: Breaking the Limits Imposed by the Low Absorbance of Dye Monolayers. *J. Phys. Chem. Lett.* **2010**, *1*, 1134–1138.
45. Buhbut, S.; Itzhakov, S.; Tauber, E.; Shalom, M.; Hod, I.; Geiger, T.; Garini, Y.; Oron, D.; Zaban, A. Built-in Quantum Dot Antennas in Dye-Sensitized Solar Cells. *ACS Nano* **2010**, *4*, 1293–1298.
46. Ko, J.; Paek, S.; Choi, H.; Kim, C.; Cho, N.; So, S.; Song, K.; Nazeeruddin, M. K. Efficient and Stable Panchromatic Squaraine Dyes for Dye-Sensitized Solar Cells. *Chem. Commun.* **2011**, *47*, 2874–2876.
47. Clifford, J. N.; Palomares, E.; Nazeeruddin, M. K.; Gratzel, M.; Nelson, J.; Li, X.; Long, N. J.; Durrant, J. R. Molecular Control of Recombination Dynamics in Dye-Sensitized Nanocrystalline TiO_2 Films: Free Energy vs Distance Dependence. *J. Am. Chem. Soc.* **2004**, *126*, 5225–5233.
48. Choi, H.; Kim, S.; Kang, S. O.; Ko, J. J.; Kang, M. S.; Clifford, J. N.; Forneli, A.; Palomares, E.; Nazeeruddin, M. K.; Gratzel, M. Stepwise Cosensitization of Nanocrystalline TiO2 Films Utilizing Al_2O_3 Layers in Dye-Sensitized Solar Cells. *Angew. Chem., Int. Ed.* **2008**, *47*, 8259–8263.
49. Kamat, P. V.; Haria, M.; Hotchandani, S. C_{60} Cluster as an Electron Shuttle in a Ru(II)-Polypyridyl Sensitizer Based Photochemical Solar Cell. *J. Phys. Chem. B* **2004**, *108*, 5166–5170.
50. Alfassi, Z. B.; Mosseri, S.; Neta, P. Reactivities of Chlorine Atoms and Peroxyl Radicals Formed in the Radiolysis of Dichloromethane. *J. Phys. Chem.* **1989**, *93*, 1380–1385.
51. Ushida, K.; Yoshida, Y.; Kozawa, T.; Tagawa, S.; Kira, A. Evidence of oxidation of aromatic Hydrocarbons by Chloromethyl Radicals: Reinvestigation of Intersolute Hole Transfer using Pulse Radiolysis. *J. Phys. Chem. A* **1999**, *103*, 4680–4689.
52. Kamat, P. V.; Das, S.; Thomas, K. G.; George, M. V. Photochemistry of Squaraine Dyes. 1. Excited Singlet, Triplet, and Redox States of Bis[4- (dimethylamino)phenyl]squaraine and bis[4-(dimethylamino)-2-hydroxyphenyl]squaraine. *J. Phys. Chem.* **1992**, *96*, 195–199.
53. Patrick, B.; George, M. V.; Kamat, P. V.; Das, S.; Thomas, K. G. Photochemistry of Squaraine Dyes. 2. Excited States and Reduced and Oxidized Forms of 4-(4-Acetyl-3,5- dimethylpyrrolium-2-ylidene)-2-(4-acetyl-3,5- dimethylpyrrol-2-yl)-3-oxocyclobut-1-en-1-olate. *J. Chem. Soc., Faraday Trans.* **1992**, *88*, 671–676.

54. Sauve, G.; Kamat, P. V.; Thomas, K. G.; Thomas, J.; Das, S.; George, M. V. Photochemistry of Squaraine Dyes: Excited Triplet State and Redox Properties of Crown Ether Squaraines. *J. Phys. Chem.* **1996**, *100*, 2117–2124.
55. Feldt, S. M.; Gibson, E. A.; Gabrielsson, E.; Sun, L.; Boschloo, G.; Hagfeldt, A. Design of Organic Dyes and Cobalt Polypyridine Redox Mediators for High-Efficiency Dye-Sensitized Solar Cells. *J. Am. Chem. Soc.* **2010**, *132*, 16714–16724.